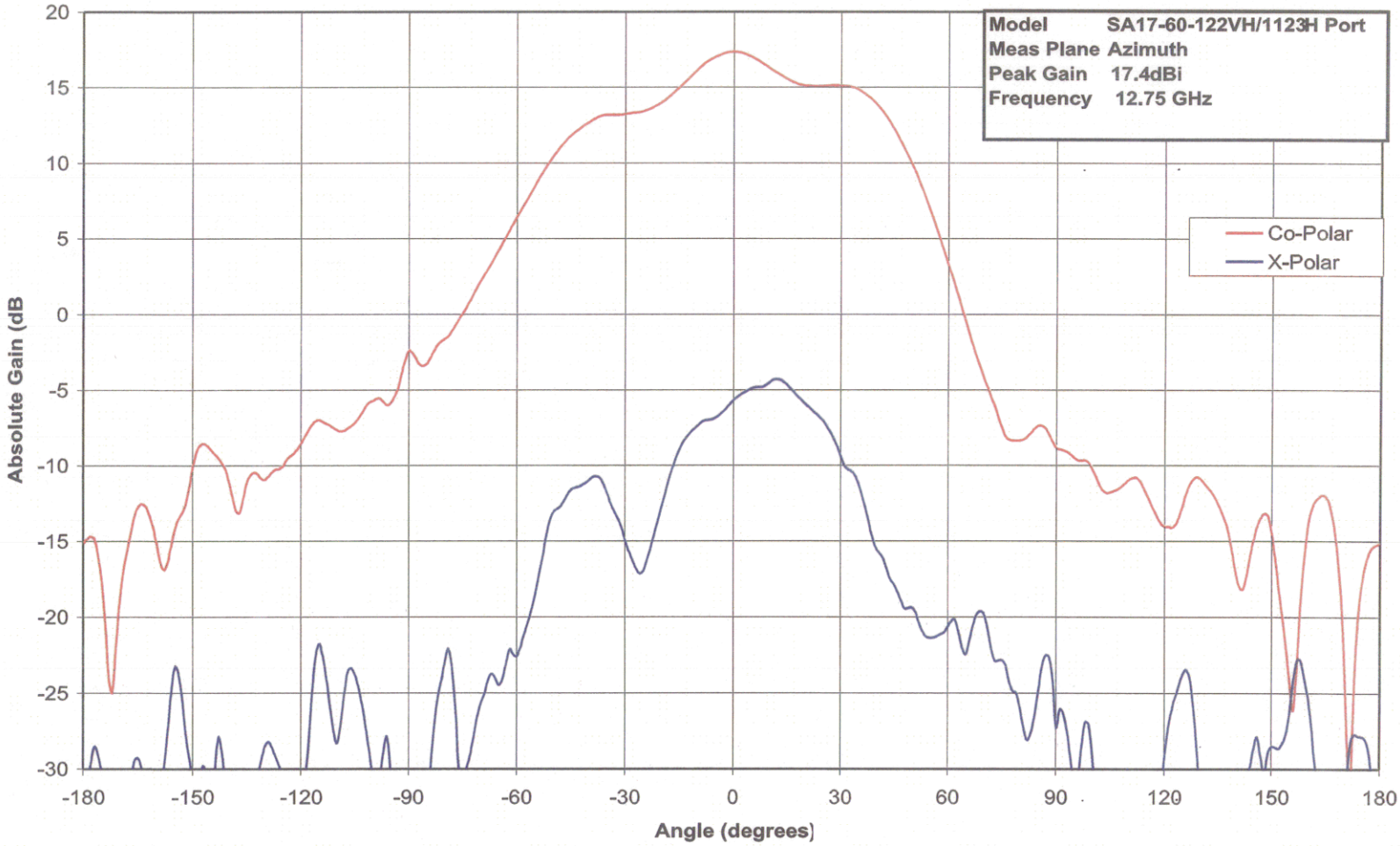

Figure 8 12.75 GHz horizontal polarization antenna - azimuthal cut

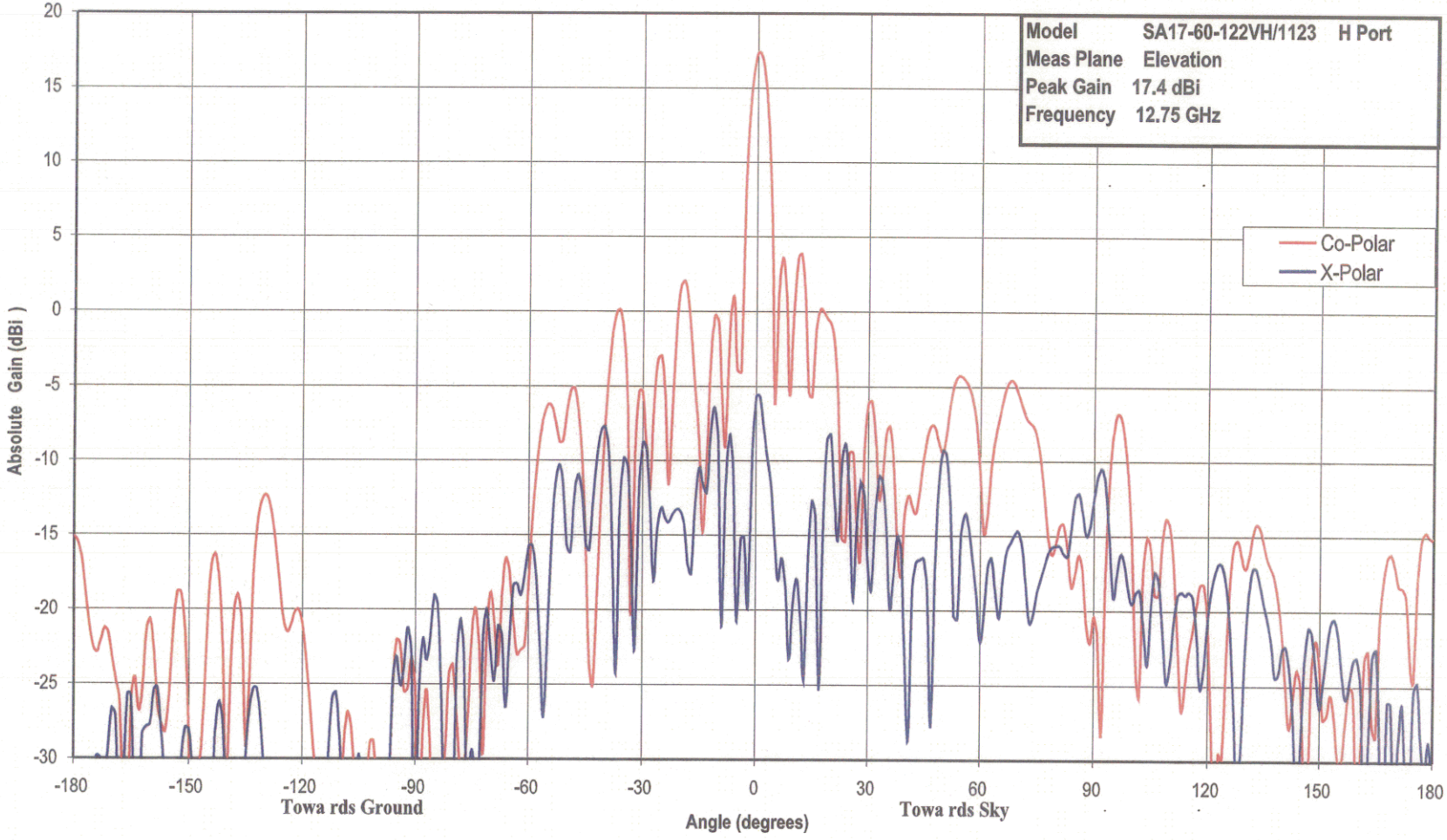

Figure 9 12.75 GHz horizontal polarization antenna - elevation cut

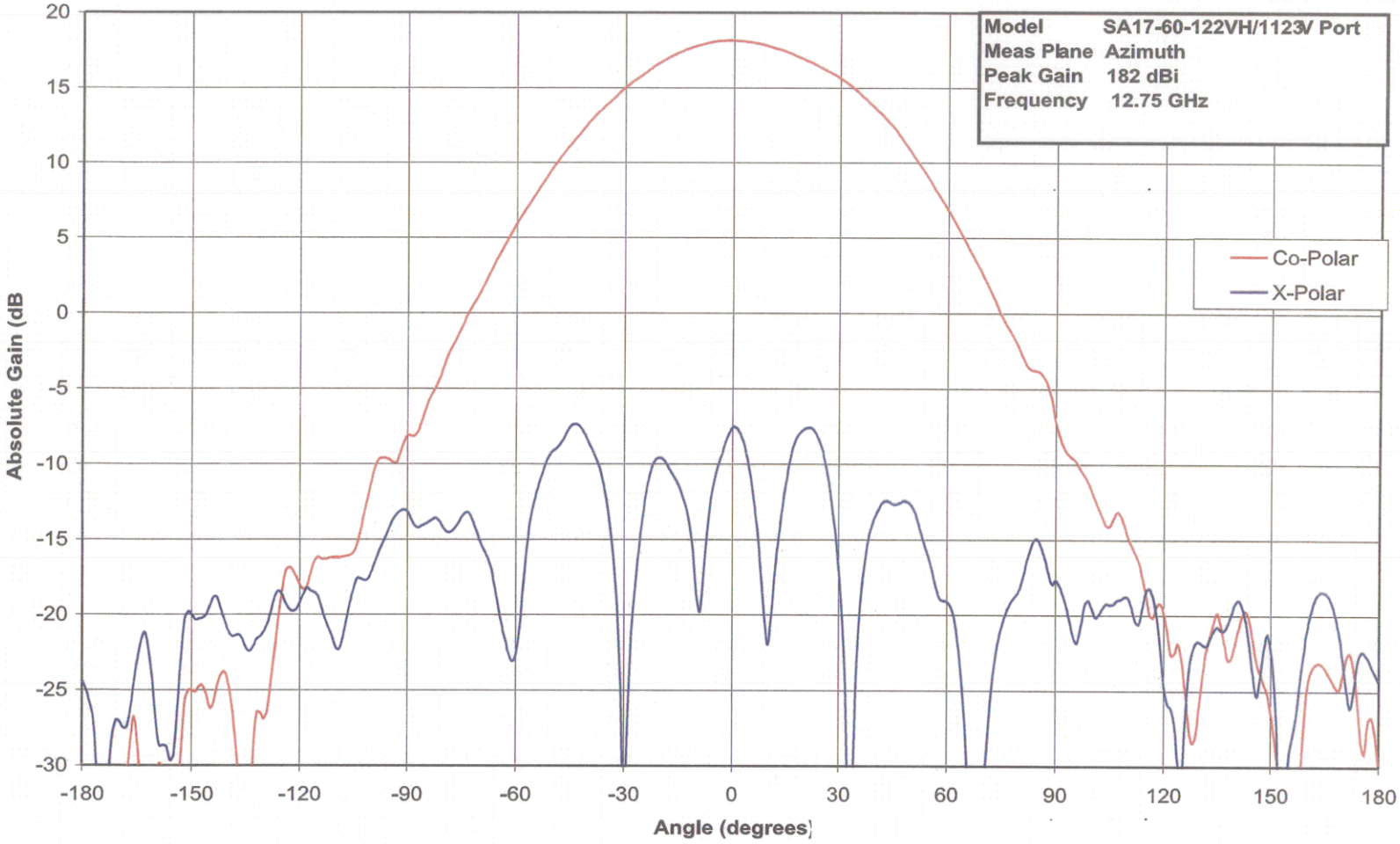

Figure 10 12.75 GHz vertical polarization antenna - azimuthal cut

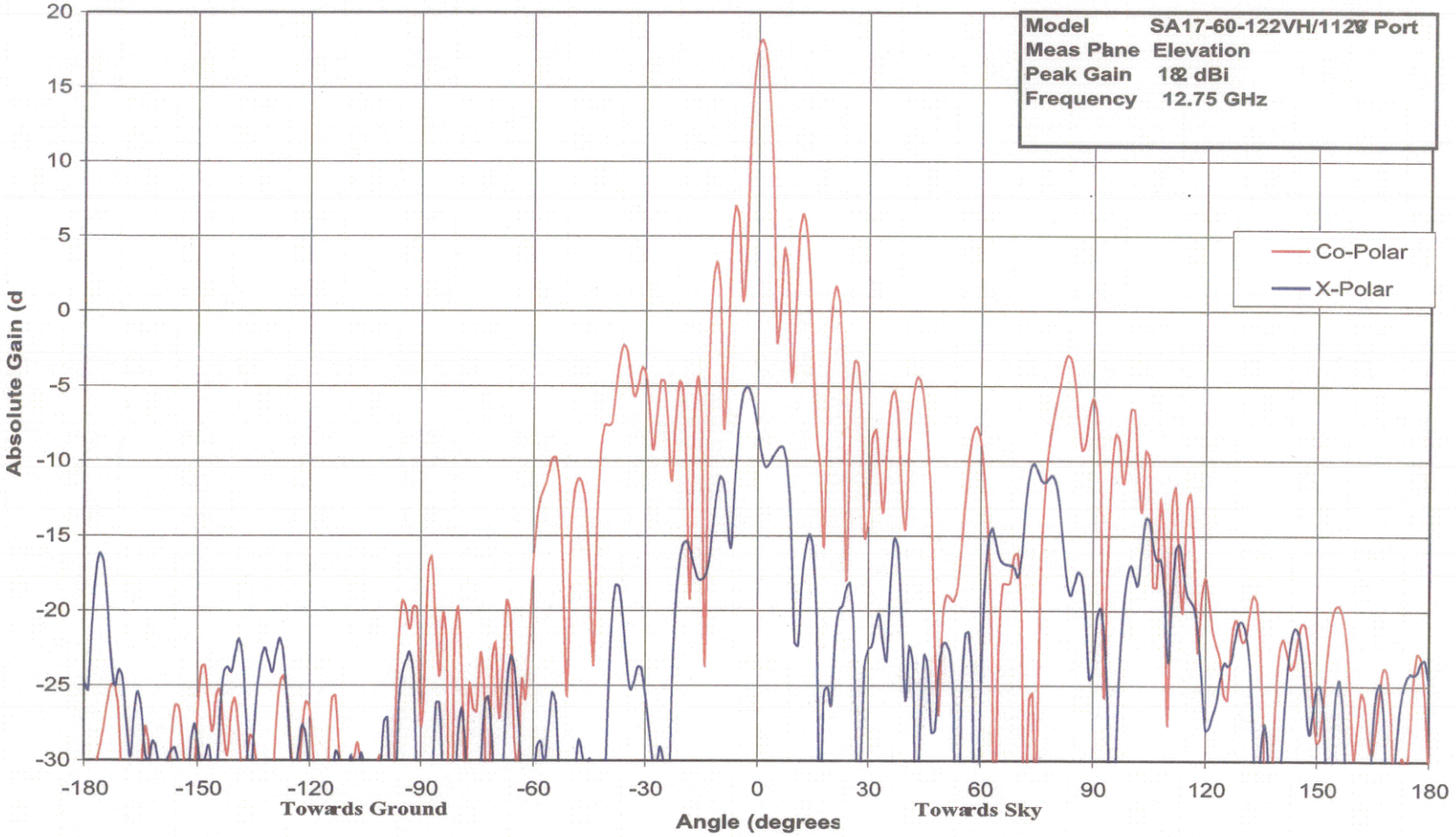

Figure 11 12.75 GHz vertical polarization antenna - elevation cut

5 Test Methodology and Procedures

The general test methodology was to measure and record changes in the DBS C/(N+I), IRD, and Bit Error Rate (BER) with the MDS transmitter ON and OFF. At each test site, the DBS receiver set is arranged to receive signal from one of the visible satellites (Sat101, Sat110, Sat119), while the calibrated test sets are arranged to receive the MDS vertical and horizontal polarization transmissions. Upon turning the MDS transmitter to ON state, a series of measurements are simultaneously made and recorded of both DBS and MDS signals, and upon turning the MDS transmitter to OFF state, another series of measurements are simultaneously made and recorded of both signals. The ON/OFF data sets for the DBS signal provide the means for comparative analysis of interference, while the ON/OFF data sets for the MDS signal provide the means for calculation of power flux density and general verification of signal present.

Test receive sites were selected with the intention to represent random variation as well as the worst-case scenarios. These sites were chosen in different directions and distances from the transmitter, including sites close to the MDS transmitter.

The measurement equipment, instrumentation, and DBS receivers were set up in two SUVs for field transportation and deployment. On one SUV a 1500 Watt DC inverter was installed so as to provide AC power for instruments within this vehicle, which included three spectrum analyzer, two D.C. power supply, a SAT 9520 installer box, a DBS receiver, and two PC compatible laptop computers, while the other SUV was used mainly for transportation of heavier equipment such as, heavy-duty tripods, DBS antennas, precision horn antennas, and various cables and tools.

The procedure for each test site was as follows:

1. Subsequent to the warm up period (30 minutes) of the spectrum analyzers, auto calibration was performed.
2. The calibrated EIRP test set antennas, the DBS antenna were positioned to receive respective signals. A GPS reading was read and recorded.
3. The DBS satellite receiver was set to receive the satellite signal.
    a. The DBS antenna was peaked using the IRD number from the SAT-9520.
    b. Carrier power was measured using a HP/4407B spectrum analyzer and recorded.
4. The MDS Transmitter was turned ON.
    a. The precision horn antennas were peaked using HP/E4407B spectrum analyzers.

b. MDS Carrier power in each polarization were measured using its' respective spectrum analyzer and recorded.

5. With the MDS transmission system ON,
   a. The satellite carrier power was measured using its' spectrum analyzer and recorded.
   b. The satellite (C/N), IRD, and BER were read from the SAT-9520 and recorded.

A site log was maintained with all the comments and notations about the sites and test conditions.

6 Test Locations

Effects of MDS transmission into the DBS shared band of MVDDS were observed at 33 locations around the MDS transmitter in Albuquerque, New Mexico. Figure 12 displays these test locations with respect to the MDS transmitter. The test location designation is intended to provide the number of separate test performed but not necessary the number of separate locations, as a number of locations required repeated measurement to ascertain the impact of MDS transmission at different power levels. Due to resolution limitation and the aforementioned fact regarding location designation, not all the test locations that are plotted in this Figure are visible. For example, test site 3 (S3) was a particularly interesting locations, since six separate test (S3, S16, S24, S26, and S33) were performed at this location on six separate occasions.

Figure 12 Receiver Test locations

As shown in Table 2, the distance between the test locations and the MDS transmitter range from 3.73 km to 37 km. This table also provides the longitude, latitude, and the height of the receiving antennas, as well as, azimuth and elevation of the test location with respect to the MDS transmitter. As shown in this table, the azimuth of the test locations range from 208° to 267° with respect to true north, while the elevation range from –2.5° to –19.4° and height from 1509 m to 1921 m over MSL.

Test Site	Latitude (Deg.)	Longitude (Deg.)	Distance to MDS TX (km)	Height (km)	Azimuth (Deg.)	Elevation (Deg.)
1	35.130515	-106.539682	12.47	1.694	219.7	-7.1
2	35.173825	-106.510897	7.16	1.817	228.0	-11.2
3	35.090320	-106.629370	21.38	1.572	229.0	-4.5
4	35.193080	-106.634477	16.75	1.530	260.9	-5.9
5	35.152815	-106.696412	23.29	1.567	252.3	-4.2
6	35.159835	-106.786337	31.00	1.773	258.3	-2.8
7	35.205443	-106.754282	27.45	1.704	267.4	-3.3
8	35.158745	-106.594145	14.42	1.579	243.4	-6.6
9	35.059403	-106.568178	20.44	1.635	211.1	-4.6
10	35.022348	-106.653105	28.31	1.519	220.3	-3.6
11	35.172348	-106.497320	6.43	1.860	219.5	-12.1
12	35.023387	-106.792502	37.69	1.718	235.4	-2.5
13A	35.208155	-106.492032	3.73	1.921	254.8	-19.4
14	35.202558	-106.504013	4.95	1.872	251.2	-15.4
15	35.077380	-106.729640	29.60	1.573	238.6	-3.3
16	35.090320	-106.629370	21.38	1.571	229.0	-4.5
17	35.023275	-106.793240	37.75	1.704	235.4	-2.5
18	35.173673	-106.510873	7.17	1.777	227.9	-11.5
19	35.079495	-106.709920	27.96	1.560	237.0	-3.6
20	35.052493	-106.678343	27.51	1.533	228.5	-3.7
21	35.026550	-106.713502	31.82	1.509	228.5	-3.2
22	35.124368	-106.666103	21.99	1.527	242.2	-4.5
23	35.056273	-106.618743	23.41	1.601	220.4	-4.1
24	35.090312	-106.629380	21.39	1.576	229.0	-4.5
25	35.122592	-106.515152	11.95	1.764	208.6	-7.1
26	35.090320	-106.629370	21.38	1.572	229.0	-4.5
27	35.077240	-106.729650	29.61	1.570	238.5	-3.4
28	35.152815	-106.696412	23.29	1.567	252.3	-4.2
29	35.173673	-106.510873	7.17	1.777	227.9	-11.5
30	35.090320	-106.629370	21.38	1.572	229.0	-4.5
31	35.022160	-106.752420	34.84	1.604	231.8	-2.8
32	35.193912	-106.631732	16.49	1.532	261.1	-6.0
33	35.090320	-106.629370	21.38	1.571	229.0	-4.5

Table 2 Receiver test locations and height

7 Data Processing

7.1 Processing of DBS Data from the Spectrum Analyzer

The output signal from the DBS antenna under test was measured using the HP/E4407B spectrum analyzer. This signal was collected using a laptop computer and the Analytic

Consulting collection software. The laptop computer has four RS-232 ports that are used to connect to three SA and a GPS, while three instances of collection software, running simultaneously, controls the communication and collection of data between the spectrum analyzers and the computer. The other two spectrum analyzers are configured to receive MDS vertical and horizontal polarization signals. As the data from the spectrum analyzers are collected on the same computer simultaneously, and as each sweep has a time stamp associated with it, the collected data can be compared and analyzed sweep by sweep across the three spectrum analyzers.

The collection software collected 401 data points after each SA sweep and recorded the data on the hard disk for later retrieval. The SA Resolution Bandwidth (RES BW) was set to one MHz for all readings, while the SA Span, Sweep (SWP), RES BW, and Video Bandwidth (VID BW) were set in such a way to allow for calibrated read out. During the data processing, one thousand sweeps were averaged, thus in the comparison plots to follow the SA data represents the average power over the number of sweeps.

As part of data processing C/N and C/(N+I) calculation were performed on the data collected from the SA configured to receive DBS signal. Calculation of C/N is based on the data obtained during the period when the MDS Transmitter was in the OFF state, while calculation of C/(N+I) is based on the data obtained during the period when the MDS Transmitter was in the ON state. In the following plots and tables, the C/N represents the ratio of power density near the center of the observed transponder to the averaged noise level immediately adjacent to the observed transponder region, while C/(N+I) represents the ratio of power density near the center of the observed transponder to the averaged noise and interference level immediately adjacent to the observed transponder region. Note that, the noise level includes the adjacent transponder interference, which has been ignored in this calculation, as they cannot be particularly isolated for this test.

In general, the noise level immediately to the left and right of a transponder differ from each other, and as a result, the ensuing calculations of C/N and C/(N+I) can differ. As such, both calculations are included for completeness and are displayed in the DBS plots around the center transponder. The C/N result is shown in blue, while C/(N+I) is shown in red.

7.2 Processing of DBS Data from the SAT-9520

The DBS output signal was measured using the Applied Instruments (AI) SAT-9520 signal meter. The SAT-9520 measures the (C/N), the Bit Error Rate (BER), and the IRD. Data was collected using a laptop computer and the AI's collection software. The AI's software collected data points approximately every 5 seconds. The data was then saved as an ASCII file on the hard disk for later retrieval.

During SAT-9520 Data Processing, every ASCII file was filtered so as to eliminate outliers and records that were poor, due to reset command inadvertently generated by the acquisition software. The outlier criteria used in the processing was the 3σ rule, which eliminates any data point that deviates from the mean by three times the standard deviation. The calculation performed on the IRD, BER, and C/N data included average and standard deviation.

7.3 Processing of MDS Data from the Spectrum Analyzer

The MDS output signal was measured using the HP/E4407B SA, and similar to DBS SA the signal was collected using a laptop computer and the Analytic Consulting collection software. MDS data processing is analogous to the processing of the DBS data, however, in this case the channel power is of prime interest instead of C/N. The computed channel power for each of the MDS channels is the 3dB channel power, which is defined to be 20 MHz wide around the center frequency. MDS channel power is computing by integrating, over the 20 MHz, the difference between MDS signal and the associated noise floor. In this way, any residual raise in the noise floor due to LNA is eliminated.

In addition, the MDS plots provide information on DBS antenna type, satellite orbital position, transponder under test, distance to the MDS transmitter, MDS EIRP, azimuth and elevation of the test location, weather condition, comments regarding test scenario, and the difference between C/N and C/(N+I).

8 Test Results

The SA measurement plots and related images are shown in Figure 15 - Figure 554 for the chronologically ranked test locations designated in Table 2 as sites 1-33. In almost all measurements of the DBS signal, using the HP/4407B SA, following setting was used:

- SPAN 100MHz
- SWP 4 msec
- RES BW 1 MHz
- VID BW 1MHz

The basic DBS results for all test site include a 100 MHz power spectrum plot centered on the observed transponder center frequency, which in nearly all sites is transponder 15, and a DBS power ratio plot corresponding to the MDS ON/OFF state. In order to compile as many data point as possible in a reasonable time, for the most part only right polarization of DBS of was observed, as the other polarization of DBS has similar behavior.

The DBS 100 MHz plots are comparison plots of the DBS power spectrum with the MDS TX ON and OFF. In addition, for almost all test sites, pair of power spectrum plots corresponding to MDS HH (Horizontal Transmit – Horizontal Receive) and MDS VV (Vertical Transmit – Vertical Receive) signals, received by the calibrated test sets, are presented. As well, an antenna configuration picture accompanies most of the results presented for each site.

As mentioned in the introduction the atmospheric conditions can significantly influence the DBS signal level as evident in some of the power spectrum plots, where there is an almost constant difference in received power levels between the two observations of DBS signal. The frequency span of this nearly constant shift in the DBS received power levels is the entire 100 MHz span of the SA. This type of atmospheric dependency of DBS signal was also observed in the Clewiston test that was carried out in 2001, where the weather conditions were extreme, with rapid change of cloud cover, temperature, and humidity, and as such a considerable number power spectrum plots demonstrated this type of syndrome. However, the weather in Albuquerque is much less humid than Clewiston with few occurrences of rapid weather change, and as a result only few power spectrum plots show significant change in the DBS signal level between the two observations. Still, it should be understood that mere constant difference of power levels over the entire 100 MHz frequency range, by itself, is not indicative of any interference or even presence of MDS signal.

A summary of the DBS measurement results obtained from SAT-9520is shown in Table 3. This table includes information regarding data collection date, site number, satellite, DBS antenna type, weather conditions, MDS transmit power, and average MDS power flux density (PFD), which is the average of H-POL and V-POL PFD, at the test site. The Sat-9520 reception

performance parameters shown in this table include average and standard deviation of IRD, C/N, and BER, as well as, the number of samples and the weather condition.

One way to understand the impact of MDS transmission on the DBS signal is to observe the change in the performance parameters collected during the OFF and ON state of MDS transmitter, ΔIRD and ΔC/N are two such measures that are calculated and shown in Table 3. Of course, when looking purely on the performance parameters, the impact of weather condition cannot be separated from the impact of MDS transmission, and as such, the value of performance measure can be limited. However, the data collected in Albuquerque had only a few power spectrum plots that showed any significant influence of atmospheric condition. As discussed below, the performance measures can be used to identify the threshold where there are no measurable indicia of MDS transmission in the DBS signal.

The DBS (C/N) calculation from the SA data processing is presented in Table 4. As mentioned earlier both the left $(C/N)_L$ and right $(C/N)_R$ signal-to-noise ratio are computed for the SA data and as such are included in this table along with their respective ΔC/N. Also included in this table are the Sat-9520 C/N and its' ΔC/N to allow easy comparison of SA C/N with Sat-9520 C/N. Additionally, this table includes some of the same supporting information that are shown in Table 3 such as data collection date, site number, satellite, DBS antenna type, weather conditions, MDS transmit power, and average MDS PFD.

8.1 Discussions

Each of the DBS power spectrum plots represents an averaging of 1000 sweeps of the spectrum analyzer. This averaging allows for detection of smallest change in the DBS signal between the two measurements, MDS ON and MDS OFF state. For example, it is possible to visually detect changes as small as 0.1 dB in the power spectrum plots, while detection of even smaller changes are possible from the actual data. Again, it should be noted that the existence of variation between the power spectrum plots is not necessarily an indication of interference by the MDS transmission, as there may be other causes, some which were discussed earlier.

Consider test site 1, located at azimuthal angle of 220° and elevation angle of –7.11° with respect to the MDS transmit site, at a distance of 12.5 km therefrom, and at a MSL of 1.69 km. Figure 15 through Figure 20 show the plots and pictures associated with this test site, where a triple LNB dish antenna is used to receive DirecTV signal from Sat101. Figure 15 and Figure 16 show respectively vertical and horizontal polarization received signal by the calibrated test sets

via the horn antennas both when the MDS transmitter is ON (shown in red) and when the MDS transmitter is OFF (shown in blue). The calculated received power of each MDS channel is displayed near the center of each channel, while the average received power and power flux density in each polarization are displayed in the legends to the right side of the graph. Also included in the legends are MDS transmitter EIRP, system gain, FSPL, and FSPL prediction for the received power based on the EIRP, system gain, and antenna pattern at 12.75 GHz. The legends further include site number, test scenario, comments (recorded during data collection), and spectrum analyzer configuration information.

Figure 17 shows the power spectrum of DBS with the MDS transmission ON (red) and the MDS transmission OFF (blue). The C/N and C/(N+I) are displayed to the left and right of TP15, which is centered on down converted center frequency of 1.178 GHz, whilst the left and right ΔC/N are displayed in the legends to the right of the graph. The other two transponders shown in this Figure, TP13 and TP17 are respectively centered at 1.148 GHz and 1.208 GHz. Some of the other information included in the legends are the site number, DBS antenna type, satellite orbital position, weather condition, and comments.

Of particular interest are the four inter-transponder regions (see Figure 17), the first of which is actually positioned outside of potential band of interference in between the down converted frequency of 1.128 GHz to 1.138 GHz. The next two inter-transponder regions are positioned to the left and right of TP15 in between the down converted frequency (L-Band) of 1.158 GHz to 1.168 GHz and in between 1.188 GHz and 1.198 GHz respectively, whilst the last inter-transponder region is position in between 1.218 GHz and 1.228 GHz. Figure 6 provides a pictorial depiction of the inter-transponder region with respect to the MDS channels in the MVDDS band. As shown in this Figure, MDS 12.407 GHz (V-POL) and 12.421 (H-POL) can directly impact the second inter-transponder region, while MDS 12.435 GHz (V-POL) and 12.45 GHz can directly impact the third inter-transponder region. In a similar fashion, MDS 12.465 GHz (V-POL) and 12.479 GHz (H-POL) can directly affect the fourth inter-transponder region. Of course, comparable relationship can be developed for the other polarization of DBS. Accordingly, an analysis of Figure 17 can now be carried out.

In the first inter-transponder region a relative difference of less than 0.1 dB is observed between the DBS traces, even as the difference in the third and fourth inter-transponder region is around 0.2 dB, while the difference in the second inter-transponder region is around 0.3 dB. The disparity in the first inter-transponder region can be attributed to normal noise deviation and/or

atmospheric variation, as this region is outside of interference band. As such, the third and fourth inter-transponder region exhibit an additional increase in the noise level of 0.1 dB above the relative difference level of the first inter-transponder region, while this additional increase is 0.2 dB for the second inter-transponder region. Accordingly, the additional increase above the relative difference level of the first inter-transponder region in the second through fourth inter-transponder region can be attributed to MDS transmission. In addition, the greater deviation associated with the second inter-transponder region can be credited to slightly greater power in the MDS 12.407 GHz channel as shown in Figure 15.

Figure 18 is the DBS power ratio plot corresponding to the MDS ON/OFF state. This graph can aid in detection of interference by providing the relative difference in dB between the two traces of DBS power spectrum corresponding to the MDS ON and OFF state. The type of divergence in the inter-transponder region, as discussed above, can also be appreciated in this Figure, however with somewhat greater difficulty, as the increase in the noise floor is not exclusive to the inter-transponder region, even though it is significantly more pronounced in this region, as will be evident in plots of other test site (see for example, site 3 plots, Figure 41 - Figure 42). In addition, the change is so minute that it is significantly lost in residual noise deviation that is still present in spite of the averaging. It should be noted that in general visual sweep by sweep examination of DBS power spectrum does not provide for detection of small interference and it is only through averaging that such minute presence can be detected.

Figure 19 show the perspective of the horn antennas toward the MDS transmitter while Figure 20 shows relative configuration of the DBS antenna with respect to the horn antennas.

Site 2 includes data from triple LNB dish antenna Sat101 and double LNB dish antenna Sat119, with the associated plots and pictures shown in Figure 21 through Figure 34. This site is 7.16 km from the transmitter site with azimuth angle of 228° and elevation angle of –11.2°. As shown in Figure 23, the DBS comparison plot for Sat101 is very similar to Figure 17 of site 1, however with slightly stronger presence of MDS transmission. The presence of MDS transmission at approximately 44 dBm can also be clearly seen in the ratio plot of Figure 24. Figure 27 and Figure 28 show respectively the comparison plot and ratio plot for Sat119. Here, strong presence of MDS transmission is also noted in both plots.

In order to determine the threshold for MDS transmission, two more sets of measurements were collected from this site on separate occasions and they are designated as site 18 and site 29. Site 18 data includes single LNB Sat101, triple LNB Sat101, double LNB

Sat110, and double LNB Sat119, all at MDS EIRP of 37 dBm, and these data are shown in Figure 215 through Figure 231. Presence of MDS can only be detected in the DBS traces of double LNB Sat119, as shown in Figure 229 and Figure 230. As mentioned above, the main beam of MDS antenna is directed at 230°, and as this location is nearly exactly along the direction of the mean beam in azimuth, significant amount energy can find its way into the DBS LNB, particularly because of the relative orientation of DBS double LNB antenna which is 145° in azimuth (i.e. spillover region).

Site 29 data includes, triple LNB Sat101, double LNB Sat110, and double LNB Sat119 for both MDS EIRP at 33 dBm and 30 dBm. The data for these scenarios are shown in Figure 443 through Figure 468. Examination of these plots show that MDS transmission does not appear to be present in any of the plots associated with MDS EIRP of 30 dBm.

Site 3 is located near the center of downtown Albuquerque at a distance of 21.4 km from the MDS transmitter with azimuthal angle of 229° and elevation angle of –4.55°. This location is at the center of the beam both in elevation and in azimuth, and as such receives the highest amount of MDS transmitted power. Furthermore, with respect to the DBS double LNB antenna, the relative azimuth angle for this site is 144°, which means there is a direct line of sight from MDS transmitter into LNBs, at the site with maximum power. As such, the MDS transmit threshold is virtually determined by the performance of this site. Given the importance of this site, five more sets of measurements were collected from this site on separate occasions and they are designated as site 16, 24, 26, 30, and 33.

Site 3 data includes triple LNB Sat101, and double LNB Sat119, for MDS EIRP of approximately 44 dBm. The results for this site are shown in Figure 35 through Figure 43. Examination of these plots show that MDS transmission does appear to be present in DBS traces of triple LNB Sat101, as shown in Figure 37 and Figure 38, and also in the traces of double LNB Sat119. Expectedly, DBS traces of double LNB Sat119 display greater presence of MDS transmission.

As discussed earlier, occasionally, the MDS transmitted power seemed somewhat out of line with the expected value, site 16 is one such instance. The results for this site are shown in Figure 175 through Figure 196. As shown in Figure 175 the average H-POL power received at this site is about 6 db higher than that predicated by FSPL, while as shown Figure 176 the difference between average received V-POL power and FSPL predicted power is about 1 dB. Evidently, the transmitted H-POL power is significantly higher than intended. The result of this